Uncertainty analysis in machine learning for lithofacies classification and porosity prediction

Runhai Feng [a*]

[a] Department of Geoscience, Aarhus University, Høegh-Guldbergs Gade 2, 8000 Aarhus C, Denmark

* Corresponding author. Email address: r.feng@geo.au.dk

SUMMARY

Recently, machine learning has been widely and successfully used by geoscientists to solve typical inverse problems. However, the uncertainty related to the learned model is not properly analysed, and sometimes a simple activation function is applied to provide posterior probability. To address this problem, variance of machine learning models is calculated that can provide additional information in the accuracy of predictions. Particularly, random forest and convolutional neural networks are used to classify lithofacies and predict porosity that are important parameters to characterize subsurface reservoirs. In the first part for lihtofacies classification, different number of trees in the ensemble forest is used to investigate its influence on the model variance. While the prediction accuracy as measured by the Matthews correlation coefficient does not change with the number of trees, nor the mean probabilities of each lithofacies. The Monte Carlo effect in the variance that arising from a limited number of bootstrap replicates can be eliminated with an increase of trees used in the forest. In the second part of porosity prediction, dropout technique is used to simulate a Bayesian network, and variance of the learned system is decomposed into two parts, in which the aleatoric uncertainty does not change with an increased number of realizations, since it accounts for the randomness in the training data that have been kept the same in the study. On the other hand, the epistemic uncertainty that reflects the variability of model parameters can be explained with an increase in the number of realizations.

Key words: Neural networks; Probability distributions; Statistic methods

1. INTRODUCTION

With the recent development with the availability of massive computational resources and assembled large datasets (Monajemi et al., 2016), machine learning has drawn many attentions inside the geoscience community, and automatic interpretation and inversion of reservoir

parameters have become applicable. Harris and Grunsky (2015) classified a lithological map in the North of Canada based on geophysical and geochemical data using random forest. A regularized full-waveform inversion has been developed by Zhang and Alkhalifah (2019), in which the facies distribution from trained neural networks is used as the prior information. Wu et al. (2019) proposed an end-to-end convolutional neural network for segmentation of seismic faults.

As an important indicator that can provide confidence in the predictions, uncertainty analysis is usually performed under the Bayesian framework (Ulrych et al., 2001). Combining available prior knowledge with information contained in the measured data (Buland and Omre, 2003), a posterior probability is commonly calculated in order to draw the range of possible values of parameters of interest. In machine learning, the probability for uncertainty analysis can be provided by majority voting score in ensemble models or with different pre-defined activation functions in neural networks (Goodfellow et al., 2016). For example, Tewari and Dwivedi (2020) compared heterogeneous ensemble methods and estimated the voting probability for the identification of geological lithofacies. Feng (2020a) applied the softmax function to compute the probability value over various possible lithofacies.

However, in the aforementioned probability calculated in machine learning, uncertainty of the learned model is not well captured, which is necessitated in decision-making problems, such as reservoir exploration or management. Random forest uses a voting score as the estimated probability (Olson and Wyner, 2018), and there is no measurement of the influence on the random forest predictions from observed training data. Bootstrap aggregation or bagging is used to reduce the variance that is usually high in a single decision tree such as classification and regression trees (Breiman, 1996), which can be conceptualized as a technique to reduce variance. So it is important to understand how the sampling variance of a bagged learner has

been changed, compared with the variance in the original model (Wager et al., 2014). In this paper, we are going to calculate the variance of random forest (Breiman, 2001) that can add additional information on the prediction accuracy. Specifically, as an important reservoir parameter (Feng et al., 2020), lithofacies is to be classified by random forest and meanwhile the classification uncertainty is analysed.

Furthermore, belonging to data-driven methods, neural networks (Goodfellow et al., 2016) have been widely used for the inversion of geophysical parameters. Goutorbe et al. (2006) applied neural networks to predict thermal conductivity from the geophysical well logs. Puzyrev (2019) inverted electromagnetic by convolutional neural networks. Das et al. (2019) proposed to use an approximated Bayesian computation method to estimate the posterior distribution of network predictions. However, the uncertainty corresponding to the neural model itself is not estimated, and additionally, the training data are uncertain due to the presence of random noises, limited training samples etc. Thus, in the second part of this paper, we use dropout, a regularization technique to prevent overfitting and co-adaptation in hidden units (Srivastava et al., 2014), to approximate the Bayesian inference for the uncertainty analysis. The proposed method is applied in a supervised porosity prediction using convolutional neural networks with different dropout ratios assigned.

The content of this paper is organized as follows: first the methodology to quantify the uncertainty in random forest for lithofacies classification and convolutional neural networks for porosity prediction is introduced; then the proposed methods are applied to numerical examples to analyse the uncertainty; finally discussion and conclusion are made.

2. METHODOLOGY

The Methodology is divided into two parts: random forest for lithofacies classification and convolutional neural networks for porosity prediction.

2.1 Random Forest in Lithofacies Classification

As an ensemble model, random forest can make a more accurate prediction than individual tree by combining predictions from multiple decision trees, and the typical overfitting problem is able to be corrected (Breiman, 2001). In classification problems, the class probability is usually computed as the fraction of samples of the same class in a leaf (Olson and Wyner, 2018). Moreover, predictions by random forest contain some errors, and prediction variability can illustrate how influential the training data for random forest predictions (Polimis et al., 2017). Thus, a new method is proposed to estimate the prediction variability, in which the variance of the forest model is calculated (Wager et al., 2014).

Bagging or bootstrapping aggregation is a popular technique to improve the stability and accuracy of statistical learners with a replacement sampling (Breiman, 1996; Wager et al., 2014). As investigated by Wager et al. (2014), the variance of bagged predictor can be estimated practically from the pre-existing bootstrap replicates of a base learner ($\hat{\theta}$) that can then be formalized as bagging version ($\hat{\theta}^{\infty}$):

$$\hat{\theta}^{\infty}(\mathrm{x}) = \mathrm{E}[f(x; Z_1^*, \cdots, Z_n^*)] \quad (1)$$

where Z_i^* is drawn independently from the original training data with a replacement sampling, i.e., it forms a bootstrap sample (Breiman, 1996; Wager et al., 2014); $f(x; Z_i^*)$ is a decision tree trained on Z_i^* with new input x to be classified; E represents the expectation with respect to the bootstrap measure (Wager et al., 2014). Generally, the expectation in eq. (1) cannot be estimated correctly, and is approximated with a Monte Carlo process by a majority voting in classification on its associated bootstrap samples:

$$\hat{\theta}^{B}(\mathrm{x}) = \underset{i}{\operatorname{argmax}} \sum_{b=1}^{B} I(f_b^*(x) = i) \tag{2}$$

in which $I(\cdot)$ is an indicator function; $f_b^*(x)$ is a classified result with input x by a decision tree trained on the b^{th} bootstrap sample ($1 \leq b \leq B$); i is a possible class. When $B \to \infty$, bagged estimator $\hat{\theta}^{\infty}$ can be perfectly recovered (Wager et al., 2014).

The interested variance of the bagged learners ($\hat{\theta}^{\infty}(\mathrm{x})$) is calculated as:

$$V(\mathrm{x}) = \mathrm{Var}[\hat{\theta}^{\infty}(\mathrm{x})] \tag{3}$$

which depends on the number B of bootstrap samples, in practice (Wager et al., 2014). Wager et al. (2014) introduced a bias-corrected version to approximate the estimator in eq. (3) with a finite number of bootstrap replicates. In random forest, individual trees are trained on bootstrap samples, and the algorithm to compute the variance of bagged predictors (eq. (3)) can be directly applied, since random forest can be regarded as bagged predictors with different base learners (Wager et al., 2014). For details in the calculation of variance of bagged predictors, please refer to Wager et al. (2014).

2.2 Convolutional Neural Networks for Porosity Prediction

Including convolutional layers as parts of its framework, convolutional neural networks (CNN) is able to learn high-level features with shared-weights architecture (Goodfellow et al., 2016). CNN was commonly used to analyse visual imageries, and has also been successfully applied in binary segmentation of seismic faults or lithofacies classification on seismic data by geophysicists (Zhao and Mukhopadhyay, 2018; Zhang et al., 2018). In this paper, CNN is applied for the prediction of porosity values in a regression process, and a supervised manner is used based on training examples from well log data. However, in a typical regression process,

only a single value can be predicted based on a set of learned hyper-parameters, in which the uncertainty in predictions is not able to be evaluated.

As proposed by Gal and Ghahramani (2016), dropout, a regularization technique for reducing overfitting (Srivastava et al., 2014), can be used to approximate the Bayesian network, and the posterior distributions can be modelled over functions. Specifically, a variational distribution of dropout mechanism ($q_{\hat{\theta}}(w)$) is selected to approximate the distribution of neural parameters given training data ($p(w|D)$), which is not mathematically tractable (Kwon et al., 2018):

$$\begin{aligned} p(y^*|x^*, D) &= \int p(y^*|x^*, w)p(w|D)dw \\ &\approx \int p(y^*|x^*, w)\, q_{\hat{\theta}}(w)dw \end{aligned} \tag{4}$$

in which $p(y^*|x^*, D)$ is the posterior distribution of model prediction y^*, given input x^* and training samples D; w is the neural parameters in the learned model.

The expectation (E) value of eq. (4) can be computed as mode average:

$$\mathrm{E}_{q_{\hat{\theta}}(y^*|x^*)}(y^*) = \frac{1}{T}\sum_{t=1}^{T} p(y^*|x^*, \widehat{w}_t) \tag{5}$$

where $\widehat{w}_t$ can be randomly drawn from the variational distribution $q_{\hat{\theta}}(w)$ in a Monte Carlo process and $q_{\hat{\theta}}(y^*|x^*)$ is a variational approximation to $p(y^*|x^*, D)$ in eq. (4) (Gal and Ghahramani, 2016; Kwon et al., 2018).

The variance (Var) of the learned model is then separated into aleatoric and epistemic parts:

$$\mathrm{Var}_{q_{\hat{\theta}}(y^*|x^*)}(y^*) \tag{6}$$

$$= \overbrace{\int \left\{ \mathrm{E}_{p(y^*|x^*,w)}(y^* y^{*T}) - [\mathrm{E}_{p(y^*|x^*,w)}(y^*)][\mathrm{E}_{p(y^*|x^*,w)}(y^*)]^T \right\} q_{\hat{\theta}}(w) dw}^{\text{aleatoric}}$$

$$+ \overbrace{\int \left\{ [\mathrm{E}_{p(y^*|x^*,w)}(y^*)][\mathrm{E}_{p(y^*|x^*,w)}(y^*)]^T - [\mathrm{E}_{q_{\hat{\theta}}(y^*|x^*)}(y^*)][\mathrm{E}_{q_{\hat{\theta}}(y^*|x^*)}(y^*)]^T \right\} q_{\hat{\theta}}(w) dw}^{\text{epistemic}}$$

where E is the expectation valued and T means the transpose operation. Particularly, the aleatoric uncertainty can account for the randomness in the training observations, and epistemic uncertainty reflects the model variability in neural parameters w (Kwon et al., 2018).

3. NUMERICAL EXAMPLE

A synthetic geological and petrophysical model created by Feng et al. (2017) is used for the demonstration in uncertainty analysis, in which the lithofacies classification and porosity predictions are performed separately.

3.1 Lithofacies Classification

The reference lithofacies of the selected subsection from the Book Cliffs model (Feng et al., 2017) is shown in Fig. 1a. The true rock properties in terms of compressibility κ ($\kappa = 1/K$, with K being the bulk modulus) and shear compliance M ($M = 1/\mu$, with μ being the shear modulus) (Feng et al., 2017) are displayed in Figs 1b and 1c, which are the inputs for the classification of lithofacies. Specifically, the inverted rock properties based on seismic data are to be used, which can exclude the location limitation of sparse wells drilled in the field.

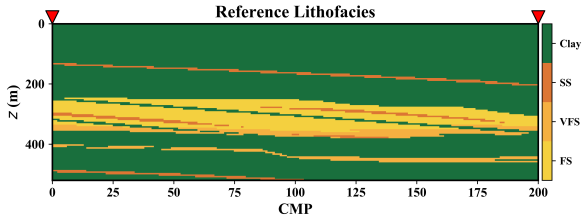

(a)

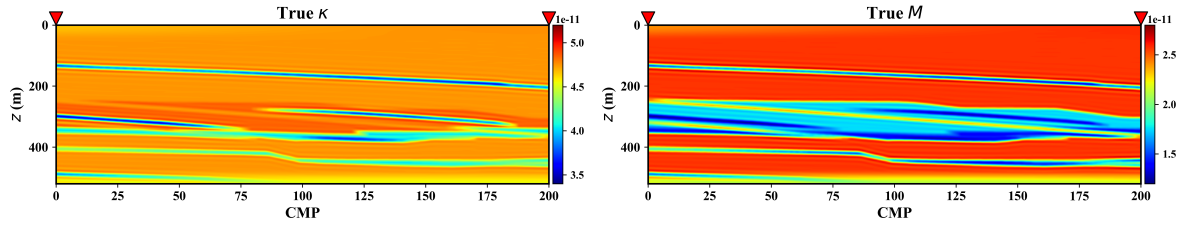

(b) (c)

Figure 1. (a) A small section of reference lithofacies from the Book Cliffs model (Feng et al., 2017). Rock properties in terms of κ (b) and M (c). The red inverse triangles are the CMP locations where the lithofacies and rock properties are used as training data for random forest.

The lithofacies and rock properties at the leftmost and rightmost CMP locations in Fig. 1 are used to train the random forest classifier. Afterwards, the inverted rock properties (Figs 2b and 3c) based on seismic data (Fig. 2a) are used as inputs for the classification of lithofacies. The seismic inversion scheme used is an elastic non-linear approach in which the internal multiples and transmissions effects are taken into account, and the pre-stack gathers are the inputs (Gisolf and Verschuur, 2010). The number of iterations determines the order of multiples used in the inversion process (Gisolf and Verschuur, 2010), and a good recovery of subsurface properties and layer geometries have been achieved (Figs 1 and 2), since the non-linear relationship between rock properties and seismic data is explored.

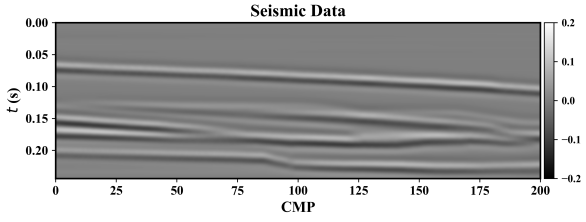

(a)

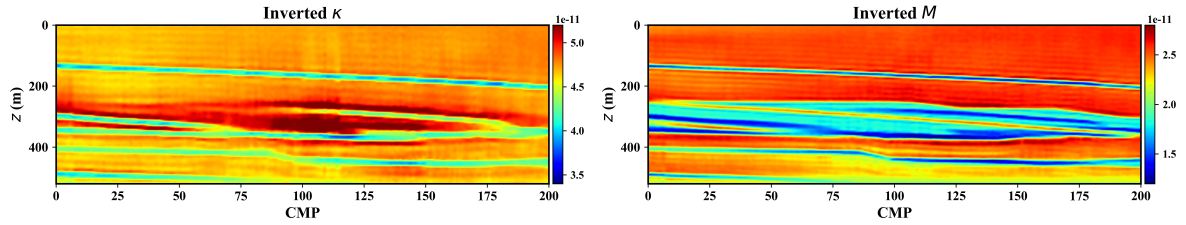

(b) (c)

Figure 2. Post-stack seismic data of the cross section after stacking the pre-stack gathers (a). Inverted κ (b) and M (c).

In random forest, the number of trees is a hyper-parameter, which can be regarded as the number of bootstrap replicates in the bagged estimator (Wager et al., 2014). Fig. 3a shows the value of Matthews correlation coefficient (MCC) (Matthews, 1975), and Fig. 3b shows the mean probability of each lithofacies by the classifier with different number of trees used in the forest. The MCC is calculated based on a multiclass confusion matrix between the reference and classified lithofacies, and its value range is between -1 (worst case) and 1 (best result).

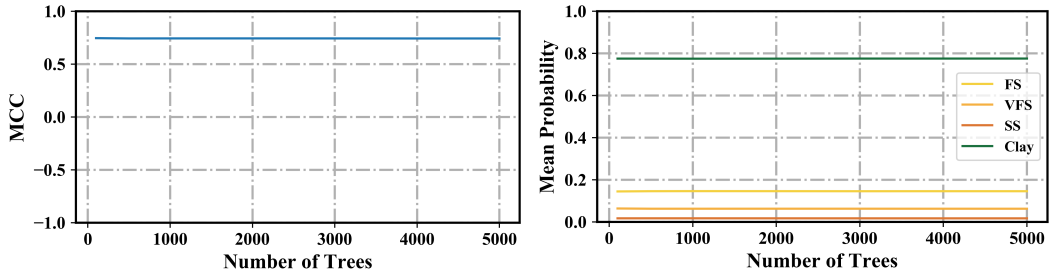

(a) (b)

Figure 3. MCC value (a) and mean probability of each lithofacies with respect to the number of trees in random forest (b). Note that MCC and mean probability are calculated for the whole cross secion.

The MCC value and mean probability of each lithofacies do not change with an increase in the number of trees, and the accuracy of lithofacies classification using seismic inversions is already high enough with a small number of trees (100).

However, as discussed in the first part in Methodology, the number of trees or the number of bootstrap replicates affects the variance of the learned model. With an increase in the number of trees used, the variance can be better explained and the Monte Carlo noises from a finite number of bootstrap replicates are reduced down to the inherent sampling errors in training data (eq. 3) (Fig. 4) (Wager et al., 2014).

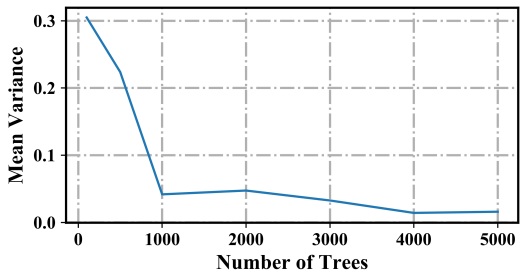

Figure 4. Mean variance with an increase in the number of trees used in random forest for the bootstrap samples.

The classified lithofacies by random forest with 5000 trees based on seismic inversions of the whole cross section (Figs 2b and 2c) are shown in Fig. 5. Compared with the reference in Fig. 1a, the lithofacies structures have been recovered quite well, even with some misclassified units, such as the discontinuous SS layers at 180 m.

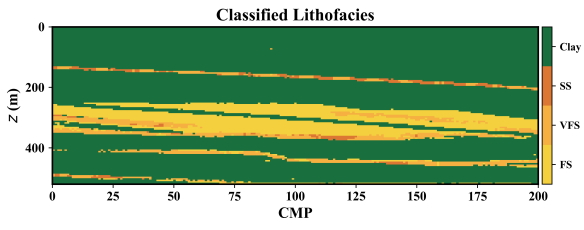

Figure 5. Classified lithofacies based on seismic inversion results (Figs 2b and 2c).

The predicted probability of each lithofacies calculated by counting the fraction of trees that vote for a certain label (Olson and Wyner, 2018) is displayed in Fig. 6, in which the uncertainty of each lithofacies at every data point can be inspected.

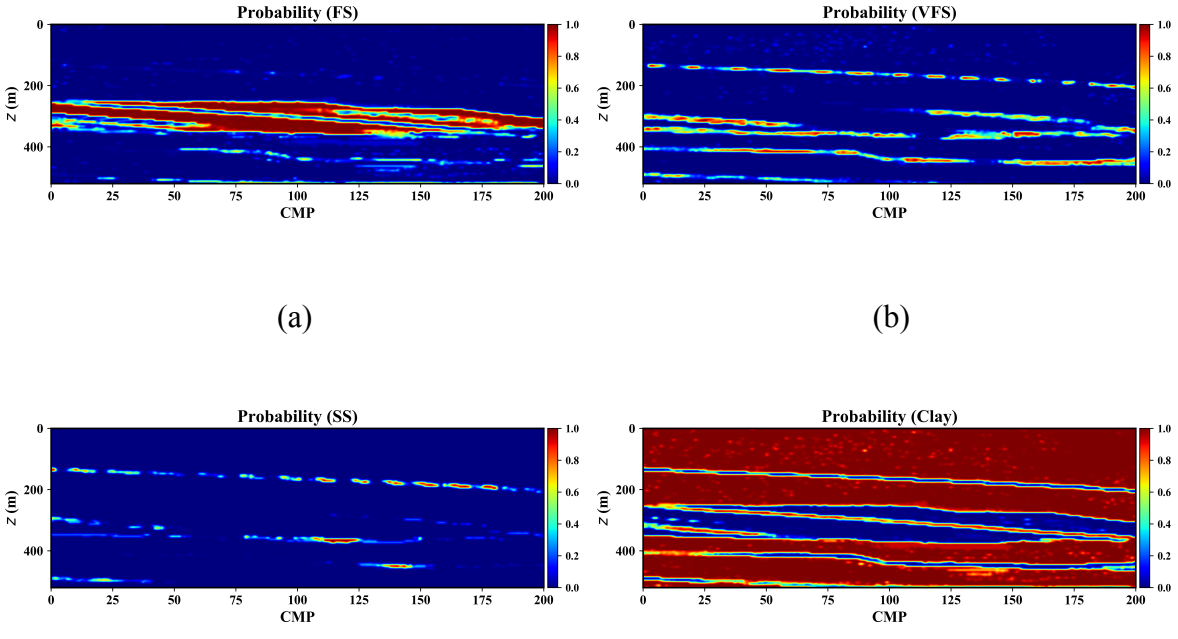

Figure 6. Predicted probability by random forest for FS (a), VFS (b), SS (c) and Clay (d).

The variance of the cross section by random forest with 5000 trees is shown in Fig. 7. Generally, Clay has a smaller variance value, and can be confidently predicted, since it has more samples in the training wells, compared with other three lithofacies (Fig. 1a).

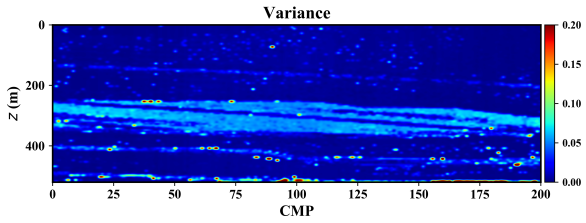

Figure 7. Variance in classification of the cross section.

3.2 Porosity Prediction

211 The second part in reservoir characterization is to predict porosity based on seismic
212 inversions. The true porosity of the selected cross section is shown in Fig. 8.

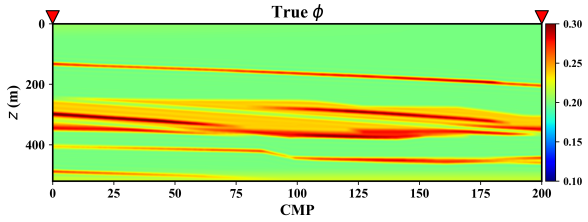

213

214 Figure 8. Ture porosity of the cross section. The inverse red triangle represents the well
215 location where the true values are used for the training of the neural model.

216 CNN model is applied for the regression of porosity values, and its network architecture is
217 the same as the one used by Feng (2020b). However, the dropout layer is added after each
218 convolutional layer to simulate the Bayesian network (Gal and Ghahramani, 2016), in which
219 two different dropout ratios are tested. After training based on the well log data (Fig. 8), the
220 seismic inversion results (Figs 2b and 2c) are used as inputs for the prediction of porosity. The
221 aleatoric and epistemic uncertainties (eq. 6) with different number of realizations are shown in
222 Fig. 9, in which the dropout ratio is 25%. The mean of aleatoric uncertainty is much larger than
223 that of the epistemic uncertainty (horizontal line in Fig. 9), which means that inherent noises
224 in the training examples take a major part in the variance, and it is not changing with an increase
225 of the realizations, since training data are kept the same in this study. The mean epistemic
226 uncertainty asymptotically converges as the number of realizations increases, which reflects
227 the variability in neural parameters that has been explained with more Monte Carlo dropout
228 simulations. Moreover, the standard deviation of aleatoric and epistemic uncertainties is
229 decreasing with an increase of realizations, as represented by vertical error bar in Fig. 9.

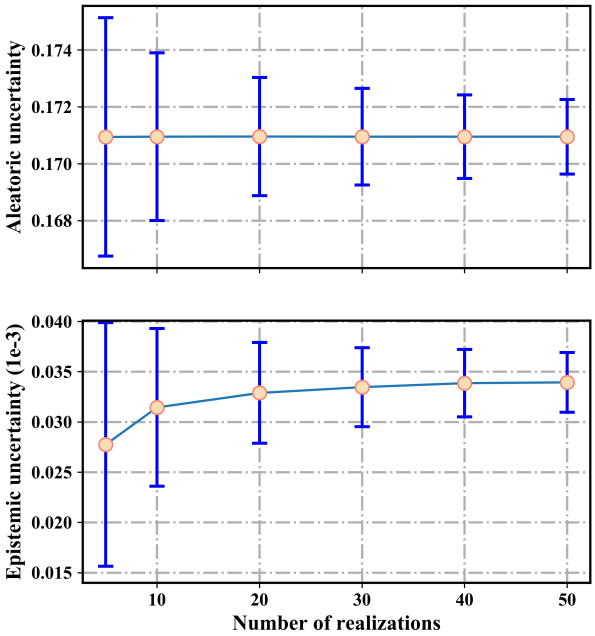

230

231 Figure 9. Aleatoric and epistemic uncertainties by CNN with a 25% dropout. The vertical
232 error bar is the standard deviation at each realization.

233 Fig. 10 shows three randomly selected realizations for the predicted porosity, and the
234 average prediction after 50 realizations which is smoothed (eq. 5), compared with the
235 independently prediction.

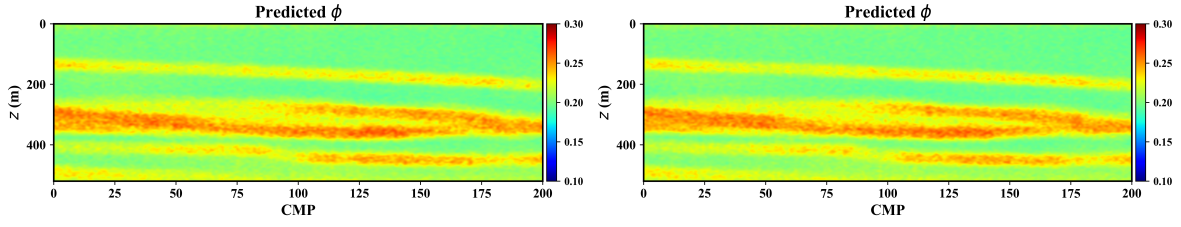

236

237 (a) (b)

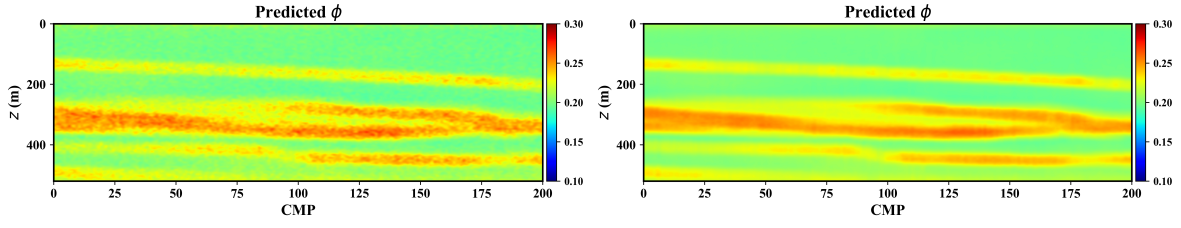

238

(c) (d)

Figure 10. (a)-(c) Three randomly selected realizations for the porosity prediction. (d) Average prediction after 50 realizations.

The total variance of aleatoric and epistemic uncertainties (eq. 6) is displayed in Fig. 11. The variance is low for porosity values that are predicted as low, which means that it is more confident in these values than other predictions, since more training examples are available at the well locations (Fig. 8).

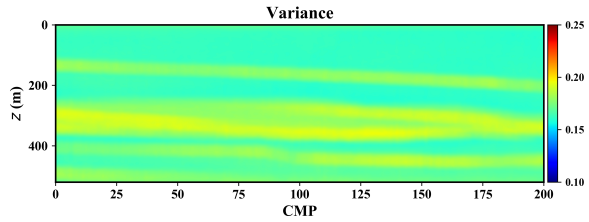

Figure 11. Variance of CNN model with a 25% dropout ratio based on 50 realizations.

Then a 50% dropout ratio is assigned in the same network. After training, the aleatoric and epistemic uncertainties for different realizations are shown in Fig. 12. Compared with the one in Fig. 9, the epistemic uncertainty is increased due to an effective dropout ratio, and the aleatoric part is almost the same.

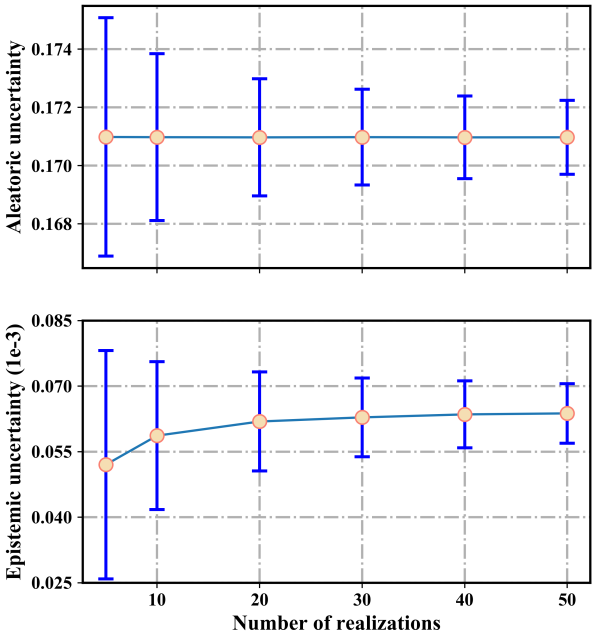

Figure 12. Aleatoric and epistemic uncertainties by CNN with a 50% dropout. Vertical error bars are the standard deviations in realizations.

The predicted porosity by averaging the 50 realizations and its associated variance are shown in Fig. 13. Notice that the variance in Fig. 13b is not too much different with the one in Fig. 11, even though the epistemic uncertainty is increased, which only takes a little part in the total variance (Fig. 12). The predicted porosity is a little higher than the one in Fig. 10d.

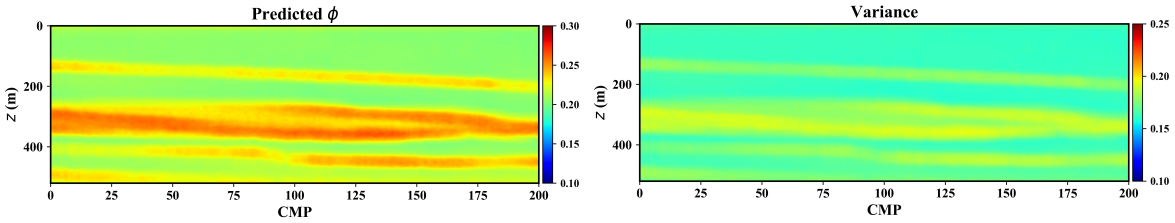

(a) (b)

Figure 13. Predicted porosity by CNN model with a 50% dropout ratio based on 50 realizations (a). Prediction variance in the cross section (b).

4. DISCUSSION

Lithofacies and porosity are important reservoir parameters for the degree qualification in subsurface compartmentalization and calculation of storage potential, not only in hydrocarbons but also for geothermal fluids (Nielsen et al., 2004). Instead of using well log data that are sparse in the field, inversion results based on seismic data are used as inputs for the characterization process, in which a non-linear inversion scheme is applied (Gisolf and Verschuur, 2010). Since the inversion scheme used is reservoir-oriented, the input seismic data should be carefully processed such as the de-migration procedure needs to be performed in order to re-datum the surface data to the reservoir target based on a selected horizon and background velocity model (Feng et al., 2017; Feng, 2020b). However, this problem has been avoided by generating the synthetic seismic data directly at the top boundary of the target model in this study (Feng et al., 2017).

As the proposed machine learning methods are supervised, lots of labelled examples are necessary for a training of the system to have a good classification and prediction performances. Two well logs in the numerical models are used, which may not be representative enough for data distributions, especially for SS samples that are too few, compared with other three lithofacies (Fig. 1a). The same problem can also be seen in the training for porosity prediction, and there are less samples for the relatively high porosity values, and more samples are available for the low porosity values, typically related with Clay (Fig. 8). A possible solution to this problem would be to generate more synthetic data samples under rock-physical modelling constraints (Das et al., 2019).

The influence of limited number in the training data for different types of lithofacies and porosity is reflected by the variance calculated in random forest and CNN (Figs 7, 11 and 13b), and generally the variance is smaller with a larger data samples available for the training, since the uncertainty associated with training examples has been better explained. And the variance

288 computed can provide an additional information regarding the prediction accuracy, rather than
289 the fraction probability calculated in the random forest, or no uncertainty information is
290 considered in the typical regression process by CNN for a porosity prediction.

291 In random forest, the number of trees used in the ensemble model is varied to inspect its
292 influence on the prediction accuracy. The MCC and mean probability of each lithofacies do
293 not change with an increased number of trees (Fig. 3), and by only using a small number of
294 trees can achieve a satisfactory accuracy. Moreover, the mean probability of lithofacies can
295 successfully imply the proportion of sampled lithofacies in the training data, or even in the
296 reference profile (Fig. 1a), with Clay taking the majority part and SS having the smallest
297 proportion. On the other hand, the number of trees affects the variance in the prediction, as its
298 value getting smaller with an increase in the number of trees used in the forest (Fig. 4). This is
299 caused by the fact that more bootstrap replicates have been used, and a more perfectly bagged
300 estimator is recovered that can account for the noises in the Monte Carlo bootstrapping process
301 (Wager et al., 2014).

302 Two different dropout ratios are used in CNN for the porosity regression, and the variance
303 that has been decomposed to aleatoric and epistemic parts (eq. 6). With an increase in the
304 number of realizations, the aleatoric uncertainty does not change, since it is associated with the
305 training data that have been kept the same, and the epistemic uncertainty can be better
306 explained with a convergent behavior (Figs 9 and 12). Compared with the ones with a 25%
307 dropout ratio (Fig. 9), the epistemic uncertainty by a 50% dropout ratio is increased, and the
308 aleatoric uncertainty is not changed that takes a major portion in the model variance (about
309 1000 times larger than the epistemic) (Fig. 12).

310 Design of network architecture and hyper-parameters tuning are important steps for a
311 successful performance of machine learning methods. A trial-and-error approach is usually

adopted to address this problem (Bishop, 2006) and the machine system with the least learning error can be used for the characterization purpose.

In a future research, a combined model is to be proposed in order to estimate lithofacies and porosity at the same. Furthermore, another important reservoir parameter, permeability, can be predicted, which indicates the pore connections in the subsurface. Then a large volume of training data is needed to train the system in a supervised manner, and the uncertainty related to the learned model has be analyzed in order to assess the confidence in the predictions.

5. CONCLUSION

Instead of using well log data, inversion results on seismic data are used as inputs in reservoir characterization, which can cover the reservoir target in a 2D or 3D way. For lithofacies classification by random forest, in addition to the probability estimated by a fraction of trees voting for certain class, the variance of bagged estimators could provide useful information in the prediction accuracy, which can be explained away given enough number of trees assigned in the ensemble forest, and then only incoherent noises in sampling data are left. On the other hand, in a typical regression problem by convolutional neural networks, there is no information for uncertainty analysis, and the dropout mechanism is used, not only in the training process but also in the prediction process, to simulate a Bayesian network. The aleatoric and epistemic uncertainties could offer additional information in the uncertainty analysis of the learned network, that can account for noises in the training examples and variability of model parameters, respectively.

Acknowledgement

This research is sponsored by the Innovation Fund Denmark in project GEOTHERM (6154-00011B) and the DELPHI Consortium.

335 **REFERENCES:**

336 Bishop, C.M., 2006. Pattern Recognition and Machine Learning. Springer.

337 Breiman, L., 1996. Bagging predictors. Machine Learning, 24 (2), 123– 140.

338 Breiman, L., 2001. Random Forests. Machine Learning, 45(1), 5-32.

339 Buland, A., Omre, H., 2003. Bayesian linearized AVO inversion. Geophysics, 68(1), 185-198,
340 doi: 10.1190/1.1543206.

341 Das, V., Pollack, A., Wollner, U., Mukerji, T., 2019. Convolutional neural network for seismic
342 impedance inversion. Geophysics, 84(6), R869–R880, doi: 10.1190/geo2018-0838.1.

343 Feng, R., Luthi, S.M., Gisolf, A., and Sharma, S., 2017. Obtaining a high-resolution geological
344 and petrophysical model from the results of reservoir-oriented elastic wave-equation based
345 seismic inversion. Petroleum Geoscience, 23, 376-385.

346 Feng, R., Balling, N., Grana, D., 2020. Lithofacies classification of a geothermal reservoir in
347 Denmark and its facies-dependent porosity estimation from seismic inversion. Geothermics,
348 87, doi: 10.1016/j.geothermics.2020.101854.

349 Feng, R., 2020a. Lithofacies classification based on a hybrid system of artificial neural
350 networks and hidden Markov models. Geophysical Journal International, 221, 1484-1498.

351 Feng, R., 2020b. Estimation of reservoir porosity based on seismic inversion results using deep
352 learning methods. Journal of Natural Gas Science and Engineering, 77, doi:
353 10.1016/j.jngse.2020.103270.

354 Gal, Y., Ghahramani, Z., 2016. Dropout as a Bayesian approximation: Representing model
355 uncertainty in deep learning. Proceedings of the 33rd International Conference on Machine

356 Learning, 48, 1050-1059.

357 Gisolf, A., Verschuur, D.J., 2010. The principles of quantitative acoustical imaging. EAGE
358 Publications b.v., Houten.

359 Goodfellow, I., Bengio, Y and Courville, A., 2016. Deep Learning, MIT Press.

360 Goutorbe, B., Lucazeau, F., Bonneville, A., 2006. Using neural networks to predict thermal
361 conductivity from geophysical well logs. Geophysical Journal International, 166, 115-125.

362 Harris, J.R., Grunsky, E.C., 2015. Predictive lithological mapping of Canada's North using
363 Random Forest classification applied to geophysical and geochemical data. Computers &
364 Geosciences 80, 9-25.

365 Kwon, Y., Won, K., Kim, B., Paik, M., 2018. Uncertainty Quantification Using Bayesian
366 Neural Networks in Classification: Application to Ischemic Stroke Lesion Segmentation.
367 International Conference on Medical Imaging with Deep Learning, Amsterdam.

368 Matthews, B. W., 1975. Comparison of the predicted and observed secondary structure of T4
369 phage lysozyme. Biochimica et Biophysica Acta (BBA) - Protein Structure 405 (2), 442-
370 451.

371 Monajemi, H., Donoho, D.L, and Stodden, V., 2016. Making massive computational
372 experiments painless. 2016 IEEE International Conference on Big Data, 2368–2373, doi:
373 10.1109/BigData.2016.7840870.

374 Nielsen, L.H., Mathiesen, A., Bidstrup, T., 2004. Geothermal energy in Denmark. Geological
375 Survey of Denmark and Greenland Bulletin, 4, 17–20.

376 Olson, M.A., Wyner, A., 2018. Making sense of random forest probabilities: a Kernel
377 perspective. arXiv:1812.05792.

Polimis, K., Rokem, A., Hazelton, B., 2017. Confidence intervals for random forests in Python. Journal of Open Source Software, doi: 10.21105/joss/00124.

Puzyrev, V., 2019. Deep learning electromagnetic inversion with convolutional neural networks. Geophysical Journal International, 218, 817-832.

Srivastava, N, Hinton, G., Krizhevsky, A., Sutskever, I., Salakhutdinov, R., 2014. Dropout: A simple way to prevent neural networks from overfitting. Journal of Machine Learning Research, 15(56), 1929-1958.

Tewari, S., and Dwivedi, U. D., 2020. A comparative study of heterogeneous ensemble methods for the identification of geological lithofacies. Journal of Petroleum Exploration and Production Technology, 10, 1849-1868.

Ulrych, T.J., Sacchi, M.D. & Woodbury, A., 2001. A Bayes tour of inversion: a tutorial. Geophysics, 66(1), 55–69.

Zhang, Z., and Alkhalifah, T., 2019. Regularized elastic full-waveform inversion using deep learning. Geophysics, doi: 10.1190/geo2018-0685.1.

Wager, S., Hastie, T., Efron, B., 2014. Confidence intervals for random forests: the Jackknife and the Infinitesimal Jackknife. Journal of Machine Learning Research, 15, 1625-1651.

Wu, X., Liang, L., Shi, Y., and Fomel, S., 2019. FaultSeg3D: Using synthetic data sets to train an end-to-end convolutional neural network for 3D seismic fault segmentation. Geophysics, 84(3), IM35-IM45, doi: 10.1190/GEO2018-0646.1.

Zhang, G., Wang, Z., Chen, Y., 2018. Deep learning for seismic lithology prediction. Geophysical Journal International, 215, 1368-1387.

399 Zhao, T., Mukhopadhyay, P., 2018. A fault-detection workflow using deep learning and image
400 processing. 88th Annual International Meeting, SEG, Expanded Abstracts, 1966–1970, doi:
401 10.1190/segam2018-2997005.1.